Coordinated Production and Utilization of $FADH_2$ by NAD(P)H−Flavin Oxidoreductase and 4-Hydroxyphenylacetate 3-Monooxygenase†

Tai Man Louie,‡,§ X. Sunney Xie,|| and Luying Xun*,‡

School of Molecular Biosciences, Washington State University, Pullman, Washington 99164-4234, and Department of Chemistry and Chemical Biology, Harvard University, Cambridge, Massachusetts 02138

Received January 16, 2003; Revised Manuscript Received April 9, 2003

ABSTRACT: 4-Hydroxyphenylacetate (4HPA) 3-monooxygenase (HpaB) is a reduced flavin adenine dinucleotide ($FADH_2$) utilizing monooxygenase. Its cosubstrate, $FADH_2$, is supplied by HpaC, an NAD(P)H−flavin oxidoreductase. Because HpaB is the first enzyme for 4HPA metabolism, $FADH_2$ production and utilization become a major metabolic event when *Escherichia coli* W grows on 4HPA. An important question is how $FADH_2$ is produced and used, as $FADH_2$ is unstable in the presence of free O_2. One solution is metabolic channeling by forming a transitory HpaB−HpaC complex. However, our in vivo and in vitro data failed to support the interaction. Further investigation pointed to an alternative scheme for HpaB to sequester $FADH_2$. The intracellular HpaB concentration was about 122 μM in 4HPA-growing cells, much higher than the total intracellular FAD concentration, and HpaB had a high affinity for $FADH_2$ (K_d of 70 nM), suggesting that most $FADH_2$ is bound to HpaB in vivo. The HpaB-bound $FADH_2$ was either used to rapidly oxidize 4HPA or slowly oxidized by O_2 to FAD and H_2O_2 in the absence of 4HPA. Thus, HpaB's high intracellular concentration, its high affinity for $FADH_2$, its property of protecting bound $FADH_2$ in the absence of 4HPA, and its ability to rapidly use $FADH_2$ to oxidize 4HPA when 4HPA is available can coordinate $FADH_2$ production and utilization by HpaB and HpaC in vivo. This type of coordination, in responding to demand, for production and utilization of labile metabolites has not been reported to date.

Escherichia coli W (ATCC 11105) can grow on 4-hydroxyphenylacetate (4HPA),[1] a common product derived from the fermentation of aromatic amino acids and some plant materials in animal intestinal tracts (*1*). 4HPA 3-monooxygenase is initially characterized as a two-component enzyme that oxidizes 4HPA to 3,4-dihydroxyphenylacetate (3,4-DHPA), initiating 4HPA metabolism in *E. coli* W (*2*). The large component (HpaB) is recently recharacterized as a novel $FADH_2$-utilizing monooxygenase that uses $FADH_2$ as a cosubstrate (*3*, *4*), and the small component (HpaC) is shown to be an NAD(P)H−flavin oxidoreductase (also known as flavin reductase) (*3*) that supplies $FADH_2$ to HpaB. The 2,4,6-trichlorophenol 4-monooxygenase of *Ralstonia eutropha* JMP134 is the second characterized $FADH_2$-utilizing monooxygenase (*5*). Sequence analysis suggests that several aromatic compound-hydroxylating enzymes are $FADH_2$-utilizing monooxygenases, involved in the biodegradation of xenobiotic compounds (*6*−*8*) or biosynthesis of antibiotics (*9*) and siderophores (*10*).

When *E. coli* W grows on 4HPA as the sole carbon and energy source, $FADH_2$ production and utilization by HpaC and HpaB become a major metabolic event. Increased free $FADH_2$ is detrimental to aerobically growing *E. coli* cells because intracellular O_2 (*11*) rapidly reacts with the unstable $FADH_2$ to produce H_2O_2, superoxide, and hydroxyl radical, causing DNA and other cellular damages (*12*−*14*). Therefore, $FADH_2$ production and utilization should be tightly coupled between HpaC and HpaB to prevent producing excessive free $FADH_2$ in vivo. Because the two-enzyme system has been only recently discovered, little is known about the coupling between HpaB and HpaC. When we tested the potential coupling between HpaC and HpaB for $FADH_2$ production and utilization in *E. coli* W, our in vitro and in vivo data did not support any apparent protein−protein interaction between HpaC and HpaB. Further investigation showed that HpaB sequestered $FADH_2$ through its high affinity for $FADH_2$. The intracellular HpaB concentration was estimated to be 122 μM in 4HPA-growing cells, suggesting that most $FADH_2$ is bound to HpaB in vivo. The HpaB-bound $FADH_2$ is either used rapidly to oxidize 4HPA (*4*) or slowly oxidized by O_2 to FAD in the absence of 4HPA; the latter was shown to significantly slow $FADH_2$ production due to a shortage of recycled FAD. Thus, the production and utilization of $FADH_2$ by HpaC and HpaB were coordinately coupled according to demand.

† This research was funded by Grant DE-FG02-00ER62891 from the NABIR program, Office of Biological and Environmental Research of the U.S. Department of Energy.

* To whom correspondence should be addressed. Phone: 509-335-2787. Fax: 509-335-1907. E-mail: xun@mail.wsu.edu.

‡ Washington State University.

§ Current address: Kemin Biotechnology, L.C., Des Moines, IA 50317-1100.

|| Harvard University.

[1] Abbreviations: FAD, flavin adenine dinucleotide; $FADH_2$, reduced FAD; NAD(P)H, reduced nicotinamide adenine dinucleotide (phosphate); flavin reductase, NAD(P)H−flavin oxidoreductase; 4HPA, 4-hydroxyphenylacetate; 3,4-DHPA, 3,4-dihydroxyphenylacetate; LB medium, Luria−Bertani medium; PCR, polymerase chain reaction; IPTG, isopropyl β-D-thiogalactopyranoside; KP_i, potassium phosphate; DTT, dithiothreitol; HPLC, high-pressure liquid chromatography; SDS−PAGE, sodium dodecyl sulfate−polyacrylamide gel electrophoresis.

10.1021/bi034092r CCC: $25.00
Published on Web 05/31/2003

Table 1: Strains and Plasmids Used in This Study

bacterium or plasmid	genotype and description[a]	ref or source
E. coli		
W (ATCC 11105)	wild type; Hpa$^+$	*2*
W-KO	*hpaC*::pTE0; Hpa$^-$	this study
DH5αpir	host for pSG76-K and pTE0; Tet^r	gift from G. Pósfai
BL21(DE3)	F$^-$ *ompT hsdS*$_B$ (r_B^- m_B^-) *gal dcm* (DE3)	Novagen
plasmids		
pSG76-K	suicidal plasmid for inactivation mutation; Km^r	*16*
pTE0	371-bp internal *hpaC* fragment in pSG76-K	this study
pTrc99A	overexpression vector; Ap^r	Pharmacia
pET30-LIC	overexpression vector; Km^r	Novagen
pHpaC	*hpaC* in pTrc99A	this study
pFre	*fre* in pTrc99A	this study
pTF2	*nmoB* in pTrc99A	*17*
pTftC	*tftC* in pTrc99A	this study
pES1	*fre* in pET30-LIC	*4*
pES2	*hpaB* in pET30-LIC	*4*
pTftC-His	N-terminal His-tagged fusion *tftC* in pET30-LIC	this study
pNmoB	*nmoB* in pET30-LIC	this study

[a] Hpa$^+$, grows on 4HPA; Hpa$^-$, does not grow on 4HPA.

Table 2: Oligonucleotide Primers Used for Construction of the *hpaC* Inactivation Mutant and Cloning of Different Flavin Reductases

primer	sequence[a]	nucleotide position	GenBank accession number
KOHpaC-F	5′-GATG**G**AATT**C**GATGAACAACGCCTGC-3′	2691−2716	Z29081
KOHpaC-R	5′-AATTGCCTGCA**G**ATCGCGGATCTC-3′	3081−3058	Z29081
HpaC-con	5′-ATGTAAGCGGTCAGGAATGG-3′	3319−3300	Z29081
pSG76-con	5′-TGTCGACAAGCTTGATCTGG-3′	55−74	Y09894
Fre-F	5′-CGGTAAA**GG**T**A**CCTGATGCGCGTT-3′	60−83	M61182
Fre-R	5′-TAGTTGCC**AAG**CTTCCCGCCTGTC-3′	867−844	M61182
HpaC-F	5′-CAACGACGA**AT**TCAACATGCTGGA-3′	2635−2658	Z29081
HpaC-R	5′-GGTTGGGCAAG**CT**TTATTCATCGG-3′	3292−3269	Z29081
TftC-F	5′-ACATATTGGTA**CC**GCTCATTCTGC-3′	772−795	U83405
TftC-R	5′-GCACAATCAG**GA**TCCATAGATAGT-3′	1474−1751	U83405
NTftC-F	5′-GACGACGACAAGATGCATGCCGGTGAAGCGGTCCAG-3′	894−915	U83405
NTftC-R	5′-GAGGAGAAGCCCGGTTCAGGCTTATTCCGCGAGCGA-3′	1437−1417	U83405
NmoB-F	5′-GTTTTGAC**CAT**ATGGCAGACCAAA-3′	1026−1003	L49438
NmoB-R	5′-GAGAGGATAGAGC**TC**ACGCCAGAG-3′	31−54	L49438

[a] The bold face indicates changes from template DNA for introduction of restriction sites. Underlined sequences of primers NTftC-F and NTftC-R were 5′ overhangs designed for ligation-independent cloning of TftC into the expression vector pET30-LIC as an N-terminal His-tagged fusion protein.

EXPERIMENTAL PROCEDURES

Materials. All reagents were purchased from Sigma, Aldrich, or Fisher. PCR primers were purchased from Gibco BRL. *Taq* DNA polymerase, restriction endonucleases, and DNA-modifying enzymes were purchased from Gibco BRL and New England Biolabs.

Strains, Plasmids, Media, and Growth Conditions. The bacterial strains and plasmids used in this study are listed in Table 1. *E. coli* strains were routinely grown at 37 °C in LB medium (*15*). *E. coli* W and its derivative strains were also grown at 30 or 37 °C in M9 minimal medium (*15*) containing thiamin (1 μg·mL^{-1}) and vitamin B_{12} (1 μg·mL^{-1}) with either 20 mM glycerol or 20 mM 4HPA as the sole carbon source. Kanamycin and ampicillin were used at 30 and 100 μg·mL^{-1}, respectively, when required. *E. coli* strains harboring overexpression plasmids were grown at 37 °C in LB medium to a turbidity of 0.6 at 600 nm before being induced by 1 mM IPTG. The culture was further incubated at room temperature with shaking for 4 h before the cells were harvested for protein purification.

Creation of the hpaC Inactivation Mutant E. coli W-KO. An internal fragment of the *hpaC* gene was amplified by PCR using primers KOHpaC-F and KOHpaC-R (Table 2) and *E. coli* W genomic DNA for 30 cycles of PCR with a thermal profile of 30 s at 94 °C, 30 s at 55 °C, and 45 s at 72 °C. The PCR product was cut by *Eco*RI and *Pst*I and then ligated into the suicidal plasmid pSG76-K (*16*) that was previously digested by *Eco*RI and *Pst*I. The ligation product was electroporated into *E. coli* DH5αpir cells, and recombinant clones were selected on LB agar supplemented with kanamycin. Plasmid DNA was extracted from these kanamycin-resistant colonies for confirmation. One plasmid, pTE0, with the correct insert was electroporated into *E. coli* W cells; homologous integration of pTE0 into the chromosome was selected on LB medium supplemented with kanamycin and confirmed by PCR with primers, pSG76-con and HpaC-con (Table 2), annealing to the plasmid and 3′ to the chromosomal *hpaC* gene, respectively.

Complementation of the hpaC Inactivation Mutant E. coli W-KO with Different Flavin Reductase Genes in Trans. Three pairs of PCR primers, Fre-F/Fre-R, HpaC-F/HpaC-R, and TftC-F/TftC-R (Table 2), were designed for cloning the *E. coli* general flavin reductase gene (*fre*) (*4*), *hpaC* of *E. coli* W (*3*), and the chlorophenol 4-monooxygenase partner flavin reductase gene (*tftC*) of *Burkholderia cepacia* AC1100

(*6*), respectively, into the expression vector pTrc99A (Amersham Pharmacia Biotech), producing plasmids pFre, pHpaC, and pTftC. The procedures were essentially the same as described for the construction of pTE0. The new plasmids and plasmid pTF2 containing the nitrilotriacetate monooxygenase partner flavin reductase gene (*nmoB*) (*17*) were electroporated into *E. coli* W-KO cells. The expression of these flavin reductase genes in *E. coli* W-KO was induced by 1 mM IPTG, when required.

Overexpression of tftC and nmoB. B. cepacia AC1100 genomic DNA and primers NTftC-F and NTftC-R (Table 2) were used to amplify *tftC* (*6*) by PCR. The PCR product was then cloned into the pET30-LIC vector by ligation-independent cloning, following the supplier's instruction (Novagen) to produce plasmid pTftC-His. The plasmid pTF2 containing *nmoB* (*17*) was used as the template for PCR amplification of the gene with primers NmoB-F and NmoB-R (Table 2). The PCR product was cut by *Nde*I and *Sst*I and then ligated into the plasmid pET30-LIC that was previously digested by *Nde*I and *Sst*I, producing plasmid pNmoB. Plasmids pTftC-His and pNmoB were subsequently transformed into *E. coli* BL21(DE3) for protein production.

Enzyme Purification. Fre and HpaB were purified from *E. coli* BL21(DE3) carrying plasmids pES1 and pES2, respectively (*4*). HpaC was purified from *E. coli* W-KO(pHpaC) by using a previously reported method (*3*). Native NmoB was purified from *E. coli* BL21(DE3)(pNmoB) grown in LB medium with 30 $\mu g \cdot mL^{-1}$ kanamycin and 3% ethanol with a previously reported method (*18*). Ethanol was added to reduce the production of NmoB in inclusion bodies (*19*). N-Terminal His-tagged fusion TftC was purified from *E. coli* BL21(DE3)(pTftC-His) cells with a previously described Ni^{2+}-NTA−agarose method (*20*). The fusion TftC eluted from the Ni^{2+}-NTA−agarose was further purified by going through a 2 mL Bio-Scale DEAE column (Bio-Rad). TftC was eluted with a 20 mL linear gradient of NaCl from 0 to 200 mM in the 20 mM KP_i buffer (pH 7.0) containing 1 mM DTT. Pure TftC was eluted off the DEAE column around 90 mM NaCl.

Enzyme Assays. FAD reductase activities were determined by monitoring the oxidation of NADH ($\epsilon_{340} = 6220\ M^{-1}\ cm^{-1}$) in 20 mM KP_i buffer (pH 7.0) containing 400 μM NADH and 10 μM FAD at 30 °C. One unit of FAD reductase activity was defined as the oxidation of 1 nmol of NADH/min. HpaB activities were determined by measuring the conversion of 4HPA to 3,4-DHPA using a reported HPLC method (*8*). The 50 μL reaction contained 20 mM KP_i buffer (pH 7.0), 200 μM 4HPA, 10 μM FAD, 2 mM NADH, various amounts of HpaB or cell extracts, and 5 units of pure Fre; the reaction was incubated at 30 °C for 1.5 min. One unit of HpaB activity was defined as the production of 1 nmol of 3,4-DHPA/min when HpaB was the limiting factor in the assay. An HpaB−HpaC coupled assay was performed with 2.0 nM HpaC and 1.9 μM HpaB in 100 μL of 20 mM KP_i buffer (pH 7.0) containing 1 mM NADH, 500 μM 4HPA, and 0.1−30 μM FAD. The reaction was incubated at 30 °C for 5 min, and the amount of 3,4-DHPA produced was measured by HPLC.

Determination of Kinetic Parameters. The apparent kinetic parameters of pure flavin reductases were determined by the FAD reductase assay. The FAD concentrations varied from 1 to 30 μM with fixed NADH concentration at 250 μM were used to determine $K_{m,FAD}$. The NADH concentrations ranging from 30 to 500 μM with fixed FAD at 10 μM were used for the measurement of $K_{m,NADH}$. Experiments were performed in triplicate, and the average initial rates were plotted against substrate concentrations. The apparent kinetic parameters were determined from the plots fitted with the equation $V_0 = (V_{max}[S]/K_M + [S])$ using the GraFit 5.0 program (Erithacus Software Ltd.).

Flavin Binding. The binding of $FADH_2$ and FAD by HpaB was measured by a size-exclusion chromatography method (*21*), which has been used to determine the binding of $FMNH_2$ by an $FMNH_2$-utilizing monooxygenase (*22*). The size-exclusion chromatography was carried out with a BioSep SEC S3000 size-exclusion column (300 by 7.8 mm, Phenomenex), equilibrated with 50 mM KP_i buffer (pH 7.0) containing 10 mM glucose, a designated concentration of $FADH_2$, 1 mM NADH, 2 $\mu g \cdot mL^{-1}$ glucose oxidase, 0.4 $\mu g \cdot mL^{-1}$ catalase, and 0.5 $\mu g \cdot mL^{-1}$ Fre at 24 °C. The buffer reservoir was continuously bubbled with N_2 gas. Glucose oxidase was used to remove trace O_2, and Fre was used to keep $FADH_2$ in the reduced form. An HPLC system (Waters) with a photodiode array detector was used for the analysis. Samples were prepared inside an anaerobic glovebox. A 5 mM $FADH_2$ stock solution was prepared by using sodium dithionite reduction. A 130 μL sample with 3.9 μM HpaB and $FADH_2$ at the same concentration as that in the running buffer was prepared in a glass vial in an anaerobic chamber (96% of N_2 and 4% of H_2). The sample vial was sealed with a rubber stopper and loaded into an autosampler (Waters). The sample (100 μL) was injected onto the column and eluted with the equilibrating buffer at 0.5 $mL \cdot min^{-1}$. Fractions of 0.5 mL were collected aerobically, and $FADH_2$ was oxidized to FAD. The samples were diluted to 2 mL with 50 mM KP_i buffer (pH 7.0) for FAD analysis by a fluorometer (LS50B, Perkin-Elmer) with an excitation wavelength of 450 nm and emission measurements at 520 nm. The FAD should be free from HpaB because of the extremely low concentrations of FAD and HpaB in the diluted sample. FAD binding was done similarly except that the running buffer was 50 mM KP_i buffer (pH 7.0) with various concentrations of FAD under aerobic conditions, and FAD was directly monitored at 450 nm by the photodiode array detector. The K_d of the HpaB−FAD complex was also determined by a spectrofluorometric titration method. The excitation wavelength was set at 280 nm, and the fluorescence emission of HpaB was recorded at 335 nm. Both excitation and emission monochromator slit widths were set at 5 nm. A 2 mL solution of 0.027 μM HpaB in 20 mM KP_i (pH 7.0) buffer was titrated with various amounts of flavin, and the change in fluorescence after each addition of flavin was recorded. The bound FAD was estimated by the equation:

$$[\text{bound FAD}] = [\text{HpaB}]\left(\frac{I_0 - I_c}{I_0 - I_f}\right) \quad (1)$$

in which [HpaB] is the initial concentration of HpaB, I_0 is the fluorescence intensity of HpaB at the initial titration point, I_c is the fluorescence intensity of HpaB at that titration point, and I_f is the fluorescence intensity at saturating concentrations of FAD. The K_d was then determined from a plot of [bound FAD] (y) vs [total FAD] (x) fitted with eq 2, using the GraFit

5.0 program. Cap is the binding capacity of HpaB.

$$y = \frac{-(K_d + x + \mathrm{Cap}) + \sqrt{(\mathrm{Cap} + x + K_d)^2 - 4x\mathrm{Cap}}}{2} \quad (2)$$

Analytical Methods. Protein concentrations were determined with a protein dye reagent (*23*) and bovine serum albumin as the standard. SDS−PAGE was done by the method of Laemmli (*24*), and gels were stained for proteins with GelCode Blue (Pierce). Size-exclusion chromatography analysis of the potential interaction between (3.9 μM) HpaB and (4 μM) HpaC was done using the same HPLC size-exclusion system as described above with 50 mM KP_i buffer (pH 7.0) as the running buffer. The cell volume of *E. coli* W growing on 4HPA was estimated with phase contrast images of *E. coli* W cells by using the public domain NIH Image Program (developed at the National Institutes of Health and available on the Internet at http://rsb.info.nih.gov/nih-image). The average dimensions were used to calculate the volume of an average cell of perfect cylinder with round ends. The relationship of turbidity at 600 nm to cell dry weight, protein in cell extract, and number of cells were determined by weighing cells collected on nitrocellulose membrane dried overnight at 105 °C, measuring the amount of protein in the cell extract, and colony counting.

RESULTS

Inactivation of hpaC in E. coli W. Plasmid pTE0, which contained a 371-bp internal fragment of *hpaC*, was electroporated into *E. coli* W cells and plated on LB agar containing kanamycin. Since pTE0 could not replicate in *E. coli* W autonomously in the absence of the Pir protein (*16*), kanamycin-resistant colonies resulted from the integration of the whole pTE0 via homologous crossover between the *hpaC* internal fragment on pTE0 and the *hpaC* gene on the chromosome, producing two truncated copies of *hpaC* on the chromosome. The integration was confirmed by PCR. One of the clones was named *E. coli* W-KO, which lost its ability to grow on 4HPA (Hpa^-) but grew on glycerol as well as the wild type (Figure 1). The Hpa^- phenotype could not be caused by a polar effect because *hpaC* is the last gene of the *hpa* cluster (*25*). Since HpaC does not directly metabolize 4HPA, the mutant must have lost the ability to supply enough $FADH_2$ for HpaB that catalyzes the first step of 4HPA catabolism in *E. coli* W (*25*).

Complementation of E. coli W-KO with Different Flavin Reductase Genes. The Hpa^- phenotype of *E. coli* W-KO was rescued when *hpaC*, *tftC*, *fre*, or *nmoB* was introduced on an expression plasmid. However, the degree of rescue depended on the gene used because the recombinant strains formed colonies on 4HPA agar at different rates (Table 3). Single colonies of the wild type, W-KO(pHpaC), and W-KO(pTftC) became visible after 48 h incubation at 30 °C. Strains W-KO(pFre) and W-KO(pTF2) did not form any colony unless they were incubated at 37 °C for 7 days. IPTG induction of cloned flavin reductase genes was required for the production of Fre, TftC, and NmoB, but not for HpaC, to allow the recombinants to grow on 4HPA (Table 3). Specific FAD reductase activities in cell extracts were measured (Table 3), confirming the expression of *fre*, *tftC*, *nmoB*, and *hpaC* from the corresponding plasmids in *E. coli* W-KO. W-KO(pHpaC) has sufficient FAD reductase activity even without IPTG induction, likely due to leaky expression of *hpaC* on the plasmid. HpaB activities were comparable in all the tested cell extracts (Table 3). The slow growth rates of W-KO(pFre) and W-KO(pTF2) were not due to the relatively low level of expression of *fre* or *nmoB* because W-KO(pTftC) had the lowest specific FAD reductase activity in its cell extract (Table 3). It appears that HpaB couples more efficiently with HpaC and TftC than with NmoB or Fre in vivo. Thus, the potential interaction between HpaB and HpaC for better $FADH_2$ transfer was investigated.

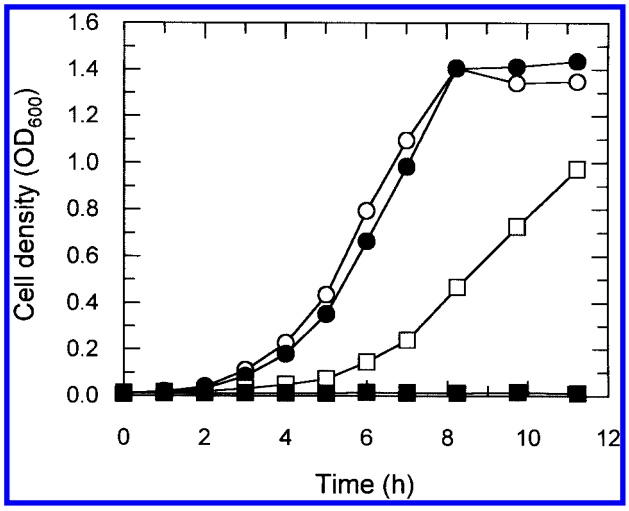

FIGURE 1: Growth curves of *E. coli* W (open symbols) and *E. coli* W-KO (solid symbols) in M9 minimal medium. Twenty millimolar glycerol (circles) or 4HPA (squares) was used as the sole carbon source at 37 °C. Experiments were repeated three times with trends consistent with data shown.

Table 3: Summary of the Growth of Different *E. coli* W-KO Strains and Specific FAD Reductase and HpaB Activities in Their Cell-Free Extracts at 30 °C

strain	carbon source	IPTG	days needed to form colonies[a]	specific activity of cell extract [nmol min^{-1} (mg of protein)$^{-1}$]	
				FAD reductase[b]	HpaB[c]
W	glycerol	no	NA[d]	76.7 ± 13.5	0[d]
W	4HPA	no	2	1046.0 ± 64.0	191
W-KO	glycerol	no	NA	80.4 ± 11.9	0
W-KO	4HPA	no	NG[d]	NA	NA
W-KO(pFre)	4HPA	yes	7	318.3 ± 61.2	144
W-KO(pFre)	4HPA	no	NG	NA	NA
W-KO(pHpaC)	4HPA	yes	2	25101.4 ± 2594.8	176
W-KO(pHpaC)	4HPA	no	2	887.7 ± 133.4	143
W-KO(pTF2)	4HPA	yes	7	265.0 ± 10.8	NT[d]
W-KO(pTF2)	4HPA	no	NG	NA	NA
W-KO(pTftC)	4HPA	yes	2	167.5 ± 24.5	196
W-KO(pTftC)	4HPA	no	NG	NA	NA

[a] Incubation was at 30 °C except for W-KO(pFre) and W-KO(pTF2) at 37 °C. [b] Average of three independent experiments with standard deviation. [c] Because the specific HpaB activities were similar, the experiment was not repeated. [d] NA, not applicable; NG, no growth; 0, undetectable activity; NT, not tested.

Analysis of the Possible Interaction between HpaB and HpaC. The possibility of direct HpaC and HpaB interaction was tested by size-exclusion chromatographic and kinetic analyses. HpaB and HpaC were subjected to size-exclusion chromatography. HpaB alone eluted off the column at 15.91 min, and HpaC alone eluted off the column at 17.66 min. If the two proteins interact to form stable complexes of larger

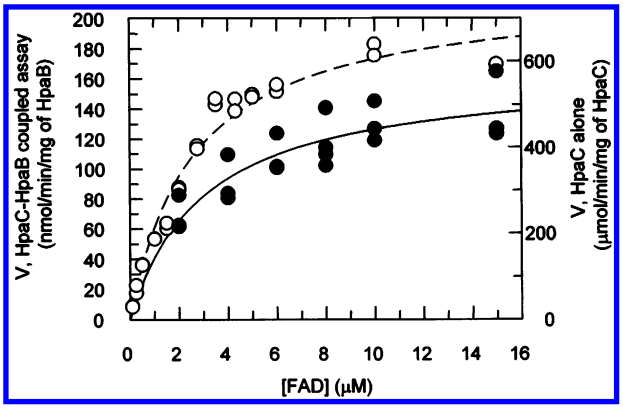

FIGURE 2: Michaelis−Menten plots of the initial rates of the HpaB−HpaC coupled assay (○) and the HpaC alone assay (●) versus FAD concentrations. In the HpaB−HpaC coupled assay, HpaB and HpaC concentrations were 2 μM and 1.9 nM, respectively. HpaC concentration in the single-enzyme assay was 9.8 nM. The K_m values of FAD in the HpaC−HpaB coupled assay and the HpaC alone assay were 2.6 ± 0.3 μM and of 3.0 ± 0.8 μM, respectively.

Table 4: Steady-State Kinetic Parameters[a] of Different Flavin Reductases Used in This Study

flavin reductase	$K_{m,FAD}$ (μM)[c]	$K_{m,NADH}$ (μM)	k_{cat} (s^{-1})	ref
Fre[b]	1.6	301	28	*39*
Fre	0.8 ± 0.1	183 ± 34	40 ± 3	this study
HpaC[b]	3.1	40	12.7	*3*
HpaC	3.0 ± 0.8	75.8 ± 6.8	178.2 ± 13.9	this study
NmoB	39.4 ± 2.8	185.5 ± 15.5	3.0 ± 0.1	this study
TftC	4.4 ± 0.8	51.3 ± 4.5	63.7 ± 4.4	this study

[a] Data were means of triplicate experiments at 30 °C with standard deviation. [b] The reported kinetic parameters of Fre and HpaC are at room temperature (*3*, *39*). [c] Determined with a fixed NADH concentration at 515 μM for Fre or 250 μM for others.

molecular size, the proteins should come off the column faster when they are run together. Yet, the retention times were unchanged when the two proteins were run together, suggesting that the two proteins do not form stable complexes under the assay conditions. Therefore, the potential for them to form transitory complexes during catalysis was tested by kinetic analysis. It has been shown that the apparent $K_{m,FMN}$ values of *Vibrio harveyi* and *Vibrio fischeri* FMN reductases decreased substantially when the assay conditions were switched from single-enzyme to luciferase-coupled assays (*26*−*28*). This decrease is due to the formation of a complex between the luciferase and the FMN reductase for the direct transfer of $FMNH_2$ (*29*). A plot of HpaB activity with FAD concentration (Figure 2) was fitted by Michaelis−Menten equation, and the apparent $K_{m,FAD}$ value of HpaC in the coupled assay with HpaB was 2.6 ± 0.3 μM, comparable to that of 3.0 ± 0.8 μM by HpaC alone (Figure 2 and Table 4). Kinetic analysis also ruled out that HpaB prefers HpaC to Fre, as the in vitro HpaB activities were very similar when the same activity unit of HpaC or Fre was used (Figure 3). These results indicate that there is no apparent protein−protein interaction between HpaC and HpaB for the transfer of $FADH_2$ under the testing conditions.

Kinetic Parameters of Flavin Reductases. To understand the coupling preference between HpaB and various flavin reductases in vivo, the kinetic parameters of the flavin reductases were determined. The four flavin reductases,

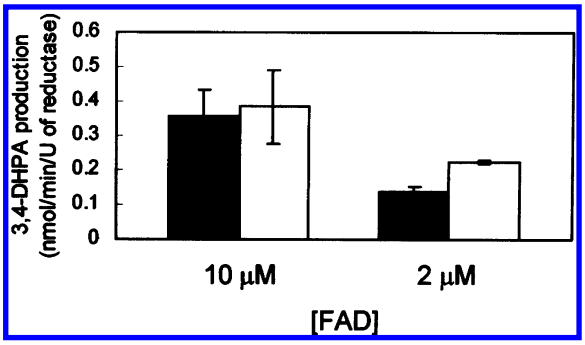

FIGURE 3: Specific HpaB activities when coupled with HpaC (black) or Fre (white) with either 2 or 10 μM FAD. The 1 mL reaction mixture in 20 mM KP_i buffer (pH 7.0) contained 0.5 mM NADH, 1 mM 4HPA, 45 units of HpaB, 45 units of either HpaC or Fre, and the specified concentrations of FAD. The reaction mixture was incubated at 30 °C, and aliquots were sampled every minute for 5 min to assay the amount of 3,4-DHPA produced. The 3,4-DHPA production rate was determined by linear regression fitting of these five data points.

HpaC, TftC, NmoB, and Fre, were purified. The apparent kinetic parameters of pure enzymes were determined with initial reaction rates of NADH oxidation in 20 mM KP_i buffer (pH 7.0) over various concentrations of FAD or NADH. The apparent high $K_{m,FAD}$ and $K_{m,NADH}$ values and low k_{cat} number of NmoB (Table 4) made the enzyme inefficient in FAD reduction. Fre was also inefficient in FAD reduction in vivo because its $K_{m,NADH}$ value (Table 4) was much larger than reported NADH concentrations, ranging from 20 to 52 μM in aerobically growing *E. coli* cells (*14*, *30*). Thus, the kinetic parameters can explain the in vivo coupling preference.

Data described so far suggest that protein−protein interaction is not required for HpaB to obtain $FADH_2$ in vitro and in vivo. To understand how HpaB sequestered $FADH_2$, the following experiments were carried out.

Flavin Binding. Size-exclusion chromatography of HpaB with various concentrations of $FADH_2$ or FAD in the running buffer under anaerobic or aerobic conditions was used to estimate the binding affinity of HpaB for $FADH_2$ or FAD. When $FADH_2$ was present in the running buffer, some $FADH_2$ coeluted with HpaB (Figure 4A). When HpaB was not present in the injected sample, all of the $FADH_2$ was eluted off the column as free $FADH_2$ (Figure 4A). The amount of $FADH_2$ coeluted with HpaB was defined as the HpaB-bound $FADH_2$ ($[FADH_2]_b$), and it was proportional to the amount of free $FADH_2$ ($[FADH_2]_f$) in the running buffer (Figure 4B). Assuming that HpaB has *n* independent binding sites for $FADH_2$ with the same affinity, a plot of $[HpaB]/[FADH_2]_b$ versus $1/[FADH_2]_f$ had a slope (K_d/n) of 0.088 and a *y*-intercept ($1/n$) of 1.25 (Figure 4C). The data were transformed into 1.6 $FADH_2$ molecules bound per dimeric HpaB and a K_d of 70 nM. Using the same approach with 0, 2.5, 5, 10, 20, and 40 μM FAD in the running buffer, we have determined the binding of HpaB to FAD as 1.3 FAD bound per dimeric HpaB with a K_d value of 6 μM. The K_d value of the HpaB−FAD complex was 5.8 ± 0.3 μM when determined by fluorometric titration, corroborating the K_d value measured by the size-exclusion method (Figure 5).

Intracellular Concentrations of HpaB and HpaC. The average volume of an *E. coli* W cell was determined to be 0.73 ± 0.19 μm^3 from the measurements of 64 cells; the

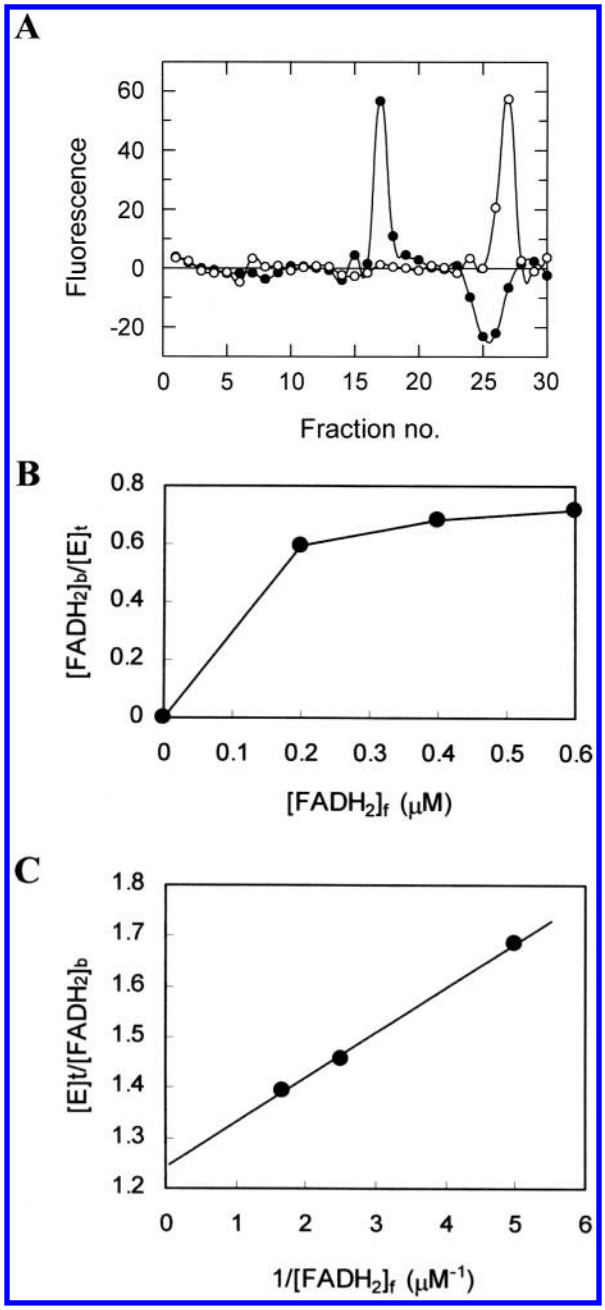

FIGURE 4: Determination of the K_d value for $FADH_2$ of HpaB by a gel exclusion method. **(**A**)** One hundred microliters of a solution containing 3.9 μM HpaB and 0.2 μM $FADH_2$ (●) was loaded onto an HPLC size-exclusion chromatography column preequilibrated and eluted with an anaerobic buffer containing 0.2 μM $FADH_2$. Fractions of 0.5 mL were collected aerobically. Upon exposure to air, $FADH_2$ was converted to FAD, which was quantified by a fluorometer. A 2.5 μM $FADH_2$ solution with no HpaB (○) was also loaded and eluted from the column under identical conditions. The peak at fraction 17 of the HpaB−$FADH_2$ run was due to HpaB-bound $FADH_2$. In the absence of HpaB, all of the $FADH_2$ was eluted as free $FADH_2$ peaked at fraction 26. **(B)** A plot of $[FADH_2]_b/[E]_t$ against $[FADH_2]_f$. $[FADH_2]_b/[E]_t$ was obtained from **(A)** and two similar runs at different $[FADH_2]_t$ in the running buffer. **(**C**)** Double reciprocal plotting of $[FADH_2]_b/[E]_t$ and $[FADH_2]_f$. Linear regression fitting ($r^2 = 0.993$) of the data had a slope of 0.088 and a *y*-intercept of 1.25 for determining K_d and the binding stoichiometry (*n*).

cell numbers were determined to be $(2.1 \pm 0.3) \times 10^9$ cells/mL of culture with a turbidity of 1 at 600 nm. There was 0.10 ± 0.01 mg of protein in cell extracts per 10^9 cells (average of nine samples with standard deviation) and 0.24 $\pm$ 0.05 mg of dry weight per 10^9 cells (average of nine samples with standard deviation). The amounts of HpaB and HpaC in cell extracts were estimated by comparing the specific enzyme activities of the cell extracts and of pure proteins, and then the concentrations inside an average cell were calculated using the determined amount of protein in cell extracts per 10^9 cells (Table 5). Our data estimated that the molar concentration of HpaB was about 8 times higher than that of HpaC in vivo. SDS−PAGE analysis of cell extracts of *E. coli* W also revealed that HpaB was a dominant protein in 4HPA-grown cells but not in glycerol-grown cells (Figure 6).

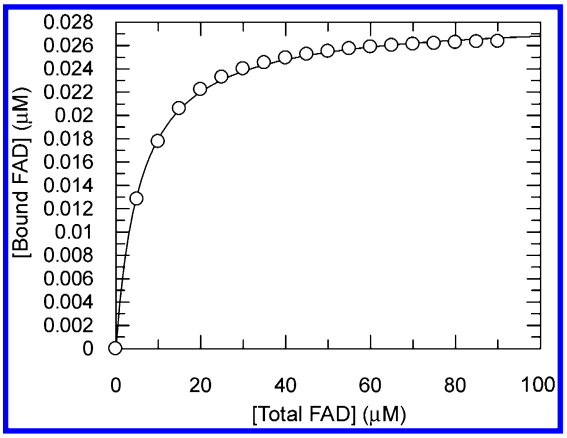

FIGURE 5: Fluorescence quenching titration of HpaB by FAD. The change in fluorescence of HpaB, due to the sequential addition of FAD (from a 10 mM stock), was converted to estimated bound FAD concentrations. The bound FAD concentrations were plotted against the total FAD concentrations. The circle (○) represents the average of three independent titrations, and the solid line represents the best-fitted titration curve (eq 2, Experimental Procedures). The K_d was calculated to be 5.8 μM from the best-fitted curve.

Effects of Excess HpaB on Flavin Reductase Activities. HpaC uses NADH to reduce FAD. FAD is rapidly regenerated from chemical oxidation of $FADH_2$ by O_2 (*4*, *12*, *13*). When HpaB was added, it slowed NADH oxidation by HpaC (Figure 7A). Since HpaB binds $FADH_2$ and slows its oxidation (*4*), the rate of NADH oxidation by HpaC is likely limited by FAD availability. This scenario was further tested by increasing HpaC concentrations in the presence or absence of excess HpaB with respect to FAD. The NADH oxidation rate increased almost linearly with the increase of HpaC, but the rate was not increased when 3.4 μM HpaB was present (Figure 7B). Similarly, excess HpaB slowed NADH oxidation by Fre (Figure 7C).

DISCUSSION

The metabolic coupling of HpaC and HpaB for $FADH_2$ production and utilization, when *E. coli* W grows on 4HPA, is investigated in this study. We initially tried to prove that protein−protein interaction was required in $FADH_2$ transfer from HpaC to HpaB. However, both in vivo and in vitro data lead us to conclude that the main route of $FADH_2$ transfer is via an alternative scheme. We will first discuss that HpaC is required to supply $FADH_2$ to HpaB in vivo, but it can be replaced by several nonhomologous flavin reductases. Then, evidence will be discussed showing that protein−protein interaction is not required for HpaB to obtain $FADH_2$. Finally and most importantly, we will discuss the evidence for the coordinated production and consumption

Table 5: Estimation of HpaB and HpaC Concentrations[a] in Strain W Cells Growing on 4HPA

protein	act. in cell extracts (units/mg)	act. of pure Hpa protein (units/mg)	Hpa protein in cell extract[b] (μg/mg)	Hpa protein in cell[c] ($\times 10^{-10}$ μg/cell)	concn in cell[d] (μM)
HpaB	191 ± 40	3400 ± 292	56 ± 13	56 ± 14	122 ± 56
HpaC	1046 ± 64	484000 ± 8000	2.2 ± 0.1	2.2 ± 0.2	16 ± 4

[a] Data were means of triplicate experiments at 30 °C with standard deviation. [b] The amount of an Hpa protein per milligram of total protein in cell extracts is calculated from its specific activities in cell extracts and the pure protein. [c] The amount of an Hpa protein per cell is calculated using a measured conversion factor from total protein in cell extracts to number of cells (0.10 ± 0.01 mg per 10^9 cells). [d] The concentration of an Hpa protein inside cells is calculated using the monomer's molecular weights of HpaB (58847.74) or HpaC (18521.51) and an average cell volume (0.73 ± 0.19 μm^3) determined from 64 cells.

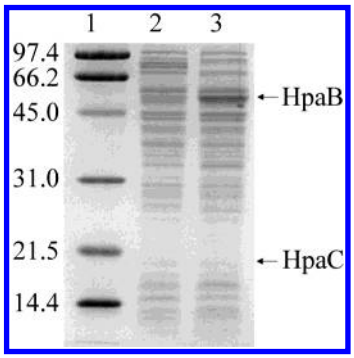

FIGURE 6: SDS−PAGE analysis of *E. coli* W cell extracts. Lanes: 1, molecular mass standards in kilodaltons (Bio-Rad); 2, 10 μg of the extract protein of *E. coli* W cells grown on glycerol; 3, 10 μg of the extract protein of *E. coli* W cells grown on 4HPA. The membrane fractions were removed by ultracentrifugation from the extracts. Arrows indicate the expected bands of HpaB and HpaC. HpaC was not a dominant protein, and its band was not visible.

of $FADH_2$ by HpaB and flavin reductases via an alternative scheme.

E. coli W-KO, an *hpaC* inactivation mutant, was unable to grow on 4HPA, indicating that HpaB requires more $FADH_2$ than the background FAD reductase activity in *E. coli* W can supply (Table 3). Fre (*31*) and NADPH−sulfite oxidoreductase, which also reduces flavins (*32*), are two reported housekeeping flavin reductases in *E. coli*. NADPH−sulfite oxidoreductase does not reduce FAD efficiently in vivo, likely because its K_m value of 81 μM for FAD (*32*) is much higher than the intracellular free FAD concentration (see below). Although FAD is the preferred substrate for Fre (*33*), Fre activities in vivo are usually quite slow due to low NADH concentrations inside aerobically growing *E. coli* cells (*14*, *30*). Therefore, the Hpa^- phenotype of *E. coli* W-KO was reverted only when the background flavin reducatase activities in *E. coli* W-KO were raised by providing HpaC, TftC, Fre, or NmoB in trans from a plasmid (Table 3).

Although HpaC (Figure 3), Fre (Figure 3), TftC (data not shown), and NmoB (data not shown) all effectively supplied $FADH_2$ for HpaB to oxidize 4HPA in vitro, they did not perform equally well in vivo. HpaC and TftC performed much better than NmoB and Fre did in vivo (Table 3). Since TftC and HpaC are 30% identical at the sequence level, it is possible that TftC has preserved the proper tertiary structural elements required for the interaction with HpaB and direct $FADH_2$ transfer. However, a more plausible explanation is based on the kinetic properties of the reductases and in vivo concentrations of NADH and FAD. NADH concentrations inside aerobically growing *E. coli* have been reported in the range of 20 (*30*) to 52 μM (*14*). The total FAD concentration (free and bound) in *Salmonella typhimurium*, a close relative of *E. coli*, is estimated to be 51 μM (*34*). The internal free FAD concentration has not been clearly defined, and only one study reports the internal free FAD concentration of *Amphibacillus xylanus* to be 13 μM (*35*). Thus, TftC and HpaC have the appropriate kinetic properties (Table 4) for efficiently producing $FADH_2$ in vivo; however, the kinetic properties of Fre and NmoB suggest that they will not be able to produce sufficient $FADH_2$ in vivo unless their protein concentrations are sufficiently high.

Several lines of in vivo and in vitro evidence suggest apparent protein−protein interaction between the HpaC−HpaB enzyme pair is not required for $FADH_2$ transfer. First, the chromosomal-encoded HpaC could be replaced by plasmid-encoded, nonhomologous flavin reductases in *E. coli* W-KO (Table 3). If a protein−protein interaction between HpaB and HpaC was required for $FADH_2$ transfer, it was unlikely that the nonhomologous flavin reductases would possess tertiary structures similar to those of HpaC, allowing them to interact with HpaB. Thus, the evidence that nonhomologous flavin reductase can replace HpaC argues against the possibility that direct protein−protein interaction is required for $FADH_2$ transfer from HpaC to HpaB in vivo. Second, using in vitro kinetic and fluorescent analyses, it has been shown that the *V. harveyi* and *V. fischeri* FMN reductases transfer $FMNH_2$ to the luciferase via protein−protein interaction (*26*−*29*). The $K_{m,FMN}$ values of *V. harveyi* and *V. fischeri* FMN reductases decreased substantially when the assay conditions were switched from single-enzyme to luciferase-coupled assays (*26*, *27*) because the turnover rate of the luciferases is much slower than that of the FMN reductases. The maximal FMN reductase activity was limited to that of the coupling luciferase in an FMN reductase−luciferase complex, and consequently 50% maximal activity of the FMN reductase−luciferase complex could be reached at much lower FMN concentrations. However, such a substantial decrease of the apparent $K_{m,FAD}$ value was not observed in the HpaC−HpaB coupled assay (Figure 2) even if the conditions of the HpaB−HpaC coupled assay were very similar to those of the FMN reductase−luciferase coupled assays (*26*, *27*). Because the apparent turnover rate of HpaB (3.3 s^{-1}), calculated from the specific activity of pure HpaB under the assay conditions (Table 5), is much lower than that of HpaC (149 s^{-1}), the lack of apparent changes in $K_{m,FAD}$ values (Figure 2) suggests that a transitory complex of HpaB and HpaC is not formed during catalysis. Third, HpaB activity was very similar no matter whether it was coupled to either HpaC or Fre in vitro (Figure 3). If HpaB preferred to receive $FADH_2$ from HpaC via direct protein−protein interaction, one would expect that HpaB activity was lower when coupled with Fre. Last, direct interaction was undetectable between HpaB and HpaC by

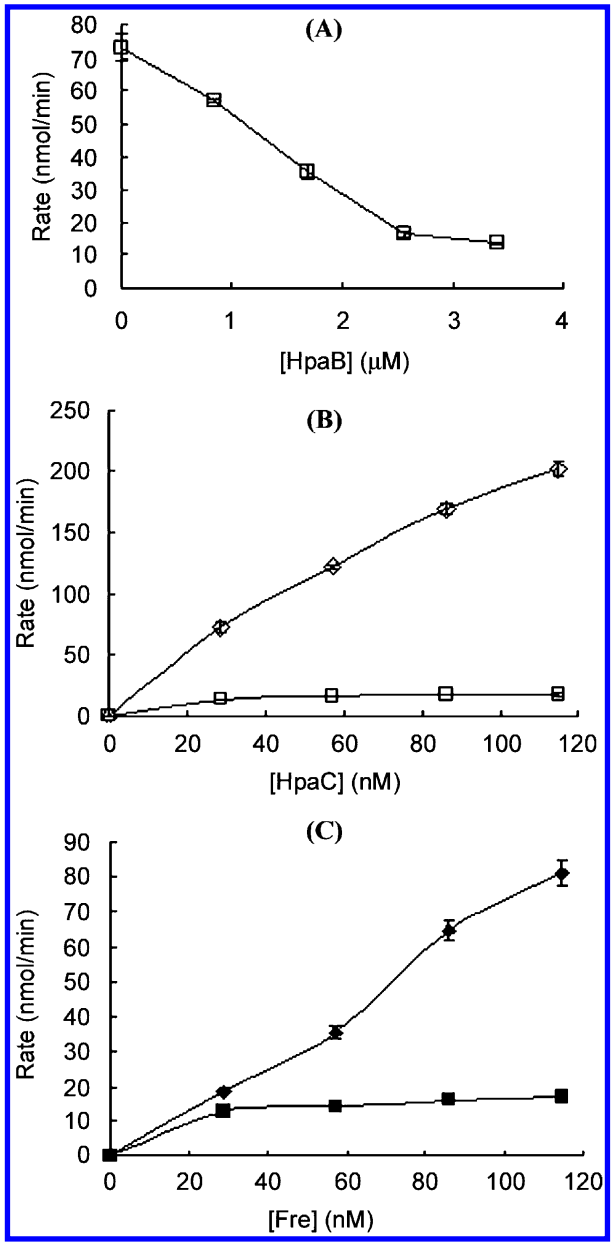

FIGURE 7: Effects of HpaB on flavin reductase activities. NADH oxidation was carried out in 0.7 mL of 20 mM KP_i buffer (pH 7.0) containing 250 μM NADH, a limiting concentration of FAD at 2 μM, and various amounts of HpaC or HpaB. **(**A**)** When the amount of HpaC was fixed at 29 nM, NADH oxidation rates were decreased by increasing HpaB in the reaction mixture. **(**B**)** NADH oxidation rates were proportional to HpaC concentrations in the reaction mixture in the absence of HpaB (◇); 3.4 μM HpaB inhibited NADH oxidation (□). **(**C**)** NADH oxidation rates were proportional to Fre concentrations in the reaction mixture in the absence of HpaB (◆); 3.4 μM HpaB inhibited NADH oxidation (■).

conventional size-exclusion chromatographic analysis. All of the data fail to support the possibility that protein−protein interaction is required for HpaB to sequester $FADH_2$.

Our data suggest that *E. coli* W manages $FADH_2$ production and utilization mainly by HpaB's high intracellular concentrations, its high affinity for $FADH_2$, and its protection of bound $FADH_2$ from rapid autoxidation. We estimated that there were 122 μM HpaB in *E. coli* W cells growing on 4HPA (Table 5), equivalent to 26800 dimeric HpaB molecules per cell. This intracellular HpaB concentration is very similar to previously reported intracellular concentrations of several proteins that catalyze major metabolic activities. (1) The periplasmic maltose-binding protein (MalE) is present at about 30000 copies per cell (*36*), (2) there are about 71000 glyceraldehyde-3-phoshpahe dehydrogenase tetramers per *E. coli* cell (*37*), and, most interestingly, (3) the luciferase concentration is 172 μM in *V. harveyi* (*29*). SDS−PAGE analysis of the whole cell extract of *E. coli* W cells grown in 4HPA (Figure 6) confirms that HpaB is a major protein inside 4HPA-grown *E. coli* W cells. This estimated HpaB concentration inside *E. coli* W cells should be about 9 times higher than the sum of free FAD and $FADH_2$, assuming their combined concentration is close to 13 μM as reported in *A. xylanus* (*35*).

HpaB has very high affinity to $FADH_2$ as estimated by a size-exclusion chromatography technique (Figure 4). Although there are no other K_d values of $FADH_2$-utilizing enzymes available for direct comparison, HpaB's K_d for $FADH_2$ (70 nM) is similar to the K_d (<80 nM) of an $FMNH_2$-utilizing monooxygenase for $FMNH_2$ (*22*). We have previously reported direct spectroscopic data for $FADH_2$ binding by HpaB, and the binding significantly slows autoxidation of $FADH_2$ in the absence of 4HPA (*4*). This phenomenon led to a shortage of FAD, regenerated from $FADH_2$ autoxidation, for flavin reductase activities (Figure 7). The reduction in flavin reductase activities is not due to the binding of FAD to HpaB because Fre's affinity for FAD (K_d of 29 nM) (*33*) is much higher than HpaB's (K_d of 6 μM). This decrease in FAD reduction rate is also not due to direct protein−protein interaction because the phenomenon occurred with both the HpaB−HpaC pair (Figure 7B) and the HpaB−Fre pair (Figure 7C). This decrease in FAD reduction rate is physiologically relevant because Figure 7B indicates that further increasing HpaC to physiological concentration (16 μM) may not significantly change the FAD reduction rate (25 nmol/min) with excess HpaB. However, the FAD reduction rate can be as high as 40000 nmol/min (extrapolated from Figure 7B) in the absence of excess HpaB. When 4HPA is available, HpaB uses O_2 to rapidly oxidize the bound $FADH_2$ and 4HPA to FAD and 3,4-DHPA, respectively. The HpaB-catalyzed oxidation of $FADH_2$ and 4HPA is at least as fast as the oxidation of free $FADH_2$ by O_2 because HpaB-bound $FADH_2$ does not accumulate in the presence of 4HPA (*4*).

Our data suggest a new in vivo scheme for $FADH_2$ production and consumption by HpaC and HpaB. *E. coli* W produces HpaB and HpaC only when 4HPA is available (Figure 6) (*38*). The intracellular HpaB concentration was 122 μM, much higher than the combined concentration (51 μM) of bound and free FAD in *S. typhimurium* (*34*), a close relative of *E. coli*. Therefore, HpaB can sequester trace amounts of $FADH_2$ in vivo because of its high concentration and its high affinity for $FADH_2$. $FADH_2$ is primarily produced by HpaC in 4HPA-growing *E. coli* W cells. The bound $FADH_2$ is immediately used to oxidize 4HPA with the concurrent regeneration of FAD, providing the substrate for HpaC to continuously produce $FADH_2$. When 4HPA becomes limited or used up, most FAD is converted to $FADH_2$, which is bound to HpaB. Due to the protective role of HpaB, the bound $FADH_2$ is only slowly oxidized back to FAD, and the lack of recycled FAD significantly decreases the rate of FAD reduction (or $FADH_2$ production) at the expense of NADH. Thus, the production and consumption of $FADH_2$ are coupled according to demand, i.e., the

availability of 4HPA. This coordinated production and utilization of a labile metabolite serve the same purpose as metabolic channeling via protein−protein interaction for labile metabolite transfer.

In conclusion, this new type of transfer of labile metabolites is at least the dominant route for HpaB to sequester $FADH_2$ in *E. coli* W, especially in the *hpaC* mutant complemented with nonhomologous flavin reductase genes. Since we did not use physiological concentrations of HpaC and HpaB to perform size-exclusion chromatography and kinetic analysis, due to technical issues dealing with very high protein concentrations, we can only conclude that no apparent protein−protein interaction occurred between HpaB and HpaC under the testing conditions. There is certainly the possibility that we simply failed to detect the protein−protein interaction by using the selected techniques and conditions. For example, the interaction of NADPH−FMN oxidoreductase and luciferase of *V. harveyi* has recently been detected by fluorescence anisotropy at low concentrations of the NADPH−FMN oxidoreductase, as the oxidoreductase dimer dissociates into monomers at low concentrations and only the monomer forms a complex with the luciferase (*29*). However, the interaction between the two proteins is predicted by kinetic analysis (*26*, *27*). Since our in vitro kinetic experiments used almost identical protein concentrations as the NADPH−FMN oxidoreductase and luciferase experiments (*26*, *27*) and failed to show any interaction, we cannot find the justification to perform the same fluorescence anisotropy experiments for HpaB and HpaC. Furthermore, the HpaB system and the luciferase system have a fundamental difference in the partner flavin reductases. HpaC does not contain any bound flavin cofactor, while the NADPH−FMN oxidoreductase of *V. harveyi* has a bound FMN cofactor. Kinetic experiments and experiments with flavin analogues showed that it is the cofactor FMN that is transferred from the NADPH−FMN oxidoreductase to the corresponding luciferase during the coupling (*26*, *27*). Since HpaC does not contain a bound FAD, the same scheme may not apply to the HpaC and HpaB pair. Thus, the NADPH−FMN oxidoreductase and luciferase form complexes for $FMNH_2$ transfer, while HpaB primarily obtains $FADH_2$ from HpaC via its high in vivo concentration and its high affinity for $FADH_2$. The ability of HpaB to slow the bound $FADH_2$ oxidation clearly plays a role to control $FADH_2$ production by HpaC or any flavin reductase when 4HPA is absent.

ACKNOWLEDGMENT

We thank Christopher M. Webster for assistance in several experiments, Erik Sandvik for creating the *hpaC* mutant, and György Pósfai of the Biological Research Center (Hungary) for the gift of plasmid pSG76-K and *E. coli* DH5αpir.

REFERENCES

1. Díaz, E., Ferrández, A., Prieto, M. A., and García, J. L. (2001) *Microbiol. Mol. Biol. Rev. 65*, 523−569.
2. Prieto, M. A., and García, J. L. (1994) *J. Biol. Chem. 269*, 22823−22829.
3. Galán, B., Díaz, E., Prieto, M. A., and García, J. L. (2000) *J. Bacteriol. 182*, 627−636.
4. Xun, L., and Sandvik, E. R. (2000) *Appl. Environ. Microbiol. 66*, 481−486.
5. Louie, T. M., Webster, C. M., and Xun, L. (2002) *J. Bacteriol. 184*, 3492−3500.
6. Hubner, A., Danganan, C. E., Xun, L., Chakrabarty, A. M., and Hendrickson, W. (1998) *Appl. Environ. Microbiol. 64*, 2086−2093.
7. Takizawa, N., Yokoyama, H., Yanagihara, K., Hatta, T., and Kiyohara, H. (1995) *J. Ferment. Bioeng. 80*, 318−326.
8. Xun, L. (1996) *J. Bacteriol. 178*, 2645−2649.
9. Delaney, S. M., Mavrodi, D. V., Bonsall, R. F., and Thomashow, L. S. (2001) *J. Bacteriol. 183*, 318−327.
10. Stintzi, A., Johnson, Z., Stonehouse, M., Ochsner, U., Meyer, J. M., Vasil, M. L., and Poole, K. (1999) *J. Bacteriol. 181*, 4118−4124.
11. Arras, T., Schirawski, J., and Unden, G. (1998) *J. Bacteriol. 180*, 2133−2136.
12. Massey, V. (1994) *J. Biol. Chem. 269*, 22459−22462.
13. Gibson, Q. H., and Hastings, J. W. (1962) *Biochem. J. 83*, 368−377.
14. Woodmansee, A. N., and Imlay, J. A. (2002) *J. Biol. Chem. 277*, 34055−34066.
15. Sambrook, J., Fritsch, E. F., and Maniatis, T. (1989) *Molecular cloning: a laboratory manual*, 2nd ed., Cold Spring Harbor Laboratory Press, Cold Spring Harbor, NY.
16. Pósfai, G., Koob, M. D., Kirkpatrick, H. A., and Blattner, F. R. (1997) *J. Bacteriol. 179*, 4426−4428.
17. Xu, Y., Mortimer, M. W., Fisher, T. S., Kahn, M. L., Brockman, F. J., and Xun, L. (1997) *J. Bacteriol. 179*, 1112−1116.
18. Uetz, T., Schneider, R., Snozzi, M., and Egli, T. (1992) *J. Bacteriol. 174*, 1179−1188.
19. Steczko, J., Donoho, G. A., Dixon, J. E., Sugimoto, T., and Axelrod, B. (1991) *Protein Expression Purif. 2*, 221−227.
20. Bohuslavek, J., Payne, J. W., Liu, Y., Bolton, H., and Xun, L. (2001) *Appl. Environ. Microbiol. 67*, 688−695.
21. Hummel, J. P., and Dreyer, W. J. (1962) *Biochim. Biophys. Acta 63*, 532−534.
22. Lei, B., and Tu, S. C. (1996) *J. Bacteriol. 178*, 5699−5705.
23. Bradford, M. M. (1976) *Anal. Biochem. 72*, 248−254.
24. Laemmli, U. K. (1970) *Nature 227*, 680−685.
25. Prieto, M. A., Díaz, E., and García, J. L. (1996) *J. Bacteriol. 178*, 111−120.
26. Lei, B., and Tu, S. C. (1998) *Biochemistry 37*, 14623−14629.
27. Jeffers, C. E., and Tu, S. (2001) *Biochemistry 40*, 1749−1754.
28. Tu, S. C., Lei, B., Liu, M., Tang, C. K., and Jeffers, C. (2000) *J. Nutr. 130* (2S), 331S−332S.
29. Jeffers, C. E., Nichols, J. C., and Tu, S. C. (2003) *Biochemistry 42*, 529−534.
30. Penfound, T., and Foster, J. W. (1996) in *Escherichia coli and Salmonella cellular and molecular biology* (Neidhardt, F. C., Ed.) pp 721−730, ASM Press, Washington, DC.
31. Fontecave, M., Eliasson, R., and Reichard, P. (1987) *J. Biol. Chem. 262*, 12325−12331.
32. Covès, J., Nivière, V., Eschenbrenner, M., and Fontecave, M. (1993) *J. Biol. Chem. 268*, 18604−18609.
33. Louie, T. M., Yang, H., Karnchanaphanurach, P., Xie, X. S., and Xun, L. (2002) *J. Biol. Chem. 277*, 39450−39455.
34. Bochner, B. R., and Ames, B. N. (1982) *J. Biol. Chem. 257*, 9759−9769.
35. Ohnishi, K., Nimura, Y., Yokoyama, K., Hidaka, M., Masaki, H., Uchimura, T., Suzuki, H., Uozumi, T., Kozaki, M., Komagata, K., and Nishino, T. (1994) *J. Biol. Chem. 269*, 31418−31423.
36. Brass, J. M., Higgins, C. F., Foley, M., Rugman, P. A., Birmingham, J., and Garland, P. B. (1986) *J. Bacteriol. 165*, 787−795.
37. Zhao, G., Pease, A. J., Bharani, N., and Winkler, M. E. (1995) *J. Bacteriol. 177*, 2804−2812.
38. Prieto, M. A., and García, J. L. (1997) *Biochem. Biophys. Res. Commun. 232*, 759−765.
39. Nivière, V., Fieschi, F., Decout, J. L., and Fontecave, M. (1999) *J. Biol. Chem. 274*, 18252−18260.

BI034092R